A Simplified Approach to Determine Airspace Complexity Maps under Automated Conflict Resolution

Erwan Salaün, Adan E. Vela, Eric Feron, John-Paul Clarke, Senay Solak[†]
Georgia Institute of Technology, Atlanta GA
[†]*University of Massachusetts, Amherst MA*

Abstract

This paper presents a new methodology for rapidly generating complexity maps for various configurations taking into account the influence of some conflict avoidance algorithm at a pair-wise intersection level. The complexity maps are based on analytical expressions, validated through simulations, of the probability of conflict and the spatial distribution of aircraft. This "closed-loop" analysis explicitly considers the role of the conflict resolution algorithm, here the offset method. It gives therefore a more realistic image of the current and future health of the considered airspace as a function of the encounter and aircraft flows characteristics. Some results of the usual "open-loop" approach are also validated, while highlighting their limitations.

Introduction

Air traffic is predicted to grow worldwide in the coming decades. In many enroute regions air traffic is expected to exceed current capacity limits, i.e. the maximum number of aircraft allowed in a given airspace, as defined by controllers. To accommodate high levels of throughput, while maintaining safety, semi-automated and fully-automated conflict resolution algorithms will be required as a support tool for the air traffic controllers [1]. One of the principle goals of the research in defining complexity maps is to objectively and accurately determine the capacity of a given element of an airspace (sector), since there are significant costs associated with miscalculating airspace capacity: an underestimated capacity leads to underutilized airspace and unnecessary holds and rerountings, whereas an overestimated capacity may lead to congestion delays or safety breaches with respect to minimum aircraft separation. This study is a first step aimed at determining the complexity of an airspace under automated conflict resolution control. In this study, we consider then with the airspace as a "closed-loop" system, where the automated conflict resolution control can be seen as the feedback loop. This method should allow air traffic managers/controllers to predict in real-time airspace complexity for a given traffic configuration (routes and flow rates characteristics), and then could be considered as an easy-to-use airspace health prediction tool for the air traffic managers.

Past research on airspace complexity and automated conflict avoidance algorithms may be considered as follows:

On the one hand, there has been a significant volume of research related to estimating air traffic complexity. In [2, 3], dynamic density is defined as a complexity metric, listing several factors that must be taken into account to evaluate the complexity of an airspace (e.g. the local density of aircraft, the number of heading, altitude and speed changes). In [4, 5], an intrinsic measure of complexity is proposed, analyzing the nonlinear dynamical system that generates the considered traffic pattern. A sectorization of the airspace based on the air traffic controller workload leads the authors of [6] to generate another kind of complexity maps. Conflict probability is certainly the complexity measure that received the most of interest in the past research studies. For instance, several tools are presented in [7, 8, 9, 10, 11, 12] to determine the probability of conflict for a given traffic geometrical configuration and flow characteristics, with and without uncertainty on the aircraft position. However, the proposed methods to compute these probabilities do not explicitly account for the existence of a conflict avoidance algorithm in the feedback loop.

On the other hand, numerous studies focused on the conflict avoidance algorithm itself, that prevent the minimum miss distance between two aircraft to be less than a given distance d (typically $d = 5$NM). If a conflict occurs, the considered algorithm allows the aircraft to do only translational shiftings (known as the

"offset method", [13, 14]), or heading changes (considering degradation in the communication, navigation and surveillance systems [15] or not [16]), or speed changes ([17, 18, 16]).

Nevertheless, very few studies deal with both aspects, i.e. generating complexity maps while accounting for the fact that the system runs in closed-loop, ie, relies on some form of conflict resolution algorithm. In [19, 20], an "input-output" approach is proposed that generates complexity maps based on the control activity required to accommodate disturbances such as the entrance of another aircraft into the airspace. However, the results presented in these papers rely on extensive simulations for the current position of aircraft and remain prohibitively time-consuming. This method is therefore not well adapted for the air traffic managers. In this paper, we propose to fill the gap between generating complexity maps in "open-loop" and considering an automated conflict resolution, as shown in Figures 1 and 2. Or in other terms, we propose to answer the two following questions: how different is the behavior of the "closed-loop" system from the behavior of the "open-loop system"? Is there a way to accurately model the influence of the conflict avoidance algorithm on the conflict? Since this paper is only a first step to answer these fundamental questions, we consider only a pairwise intersection between aircraft flows flying along two straight lines. Further developments will extend this approach to a more realistic airspace with N intersecting flows.

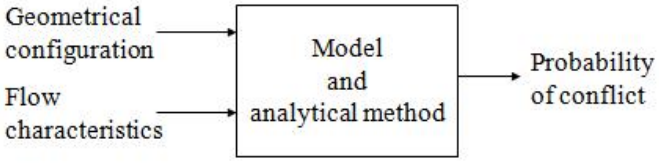

Figure 1: "Open-loop" System Analysis

The paper is organized as follows. First, we present the encounter modeling and the considered conflict avoidance algorithm (the offset method). In the next section, we present an "open-loop" analysis to rapidly determine the probability of conflict as a function of the encounter and flows characteristics and compare the results with the "closed-loop" results from simulations. Then, we propose a simplified model to capture the main behaviors of the "closed-loop" system and validate this model through extensive simulations. And at last, we present our conclusions and future works.

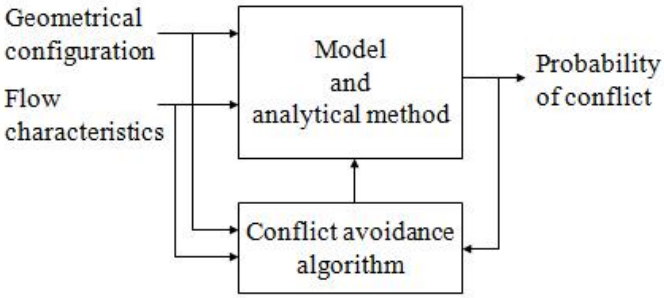

Figure 2: "Closed-loop" System Analysis

Encounter Modeling and Conflict Avoidance Algorithm

To model the encounter between two aircraft, as well as the automated conflict avoidance algorithm (the "offset method"), we use an approach similar to the work presented in [21] and [14]. The reader is therefore referred to [21, 14] for further justifications on the assumptions we make in this article. We consider the intersection between two aircraft streams: the stream 1 from West, and the stream 2 in a given circular control surface $\mathscr{C}$ corresponding to the conflict management area (see Fig. 3). All the aircraft we consider are in the conflict area (either entering $\mathscr{C}$ or already inside $\mathscr{C}$). However, to improve readability, we often do not specify it. The two straight-line tracks intersect at the point O with an angle θ. Prior to the conflict management area, the aircraft fly aligned along one of the two straight-line tracks. For $i = 1,2$, let AC_i^k be the kth aircraft of the flow i, where $k = 1$ corresponds to the *last* aircraft entering the conflict area. Each flow is characterized by the velocity vector $\mathbf{v_i}$ of each aircraft (we assume that all aircraft from stream 1 and stream 2 are flying at the same speed v), and by the probability density function $f_{\Delta T_i}(\Delta t_i)$ of the inter-arrival time Δt_i between aircraft from flow i.

Considering any pair of aircraft AC_i^k and AC_j^l, there is a conflict if the minimum miss distance between these two aircraft is strictly less than d (typically $d = 5$NM). To avoid conflict between aircraft in the same flow before crossing $\mathscr{C}$, we assume that $f_{\Delta T_i}(\Delta t_i)$ is such that $\Delta t_i \geq \frac{d}{v}$. According to [13], aircraft AC_i^k and AC_j^l from

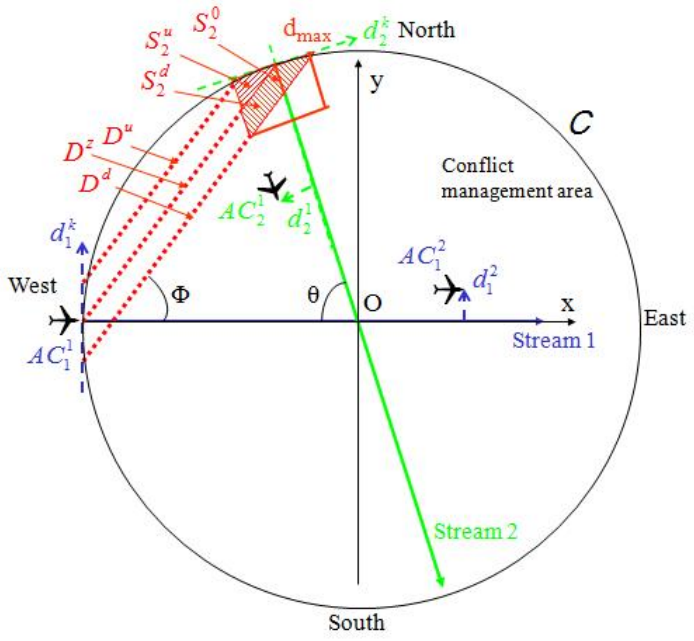

Figure 3: Encounter and Avoidance Algorithm Modeling

different flows ($i \neq j$) are not in conflict if and only if

$$-x_i^k \tan\phi + y_i^k \geq -x_j^l \tan\phi + y_j^l + \frac{d}{\cos\phi} \quad (1)$$

$$-x_i^k \tan\phi + y_i^k \leq -x_j^l \tan\phi + y_j^l - \frac{d}{\cos\phi} \quad (2)$$

where ϕ is the angle between the relative vector $\mathbf{v_i} - \mathbf{v_j}$ and $\mathbf{v_i}$, i.e. $\phi = \frac{\pi}{2} - \frac{\theta}{2}$. If we consider AC_1^1 entering in the conflict management area, a conflict occurs if there is any aircraft from stream 2 located between the straight lines D^u and D^d (see Fig. 3). If a conflict occurs, only the aircraft entering $\mathscr{C}$ can be subject to an avoidance maneuver. We consider in this article the offset model for conflict avoidance: AC_i^k performs a lateral maneuver of amplitude d_i^k at the conflict management area entrance ($d_i^k = 0$ if there is no conflict) while its speed and its heading remain the same before and after the position change. In [13], it is established that the lateral deviation of any aircraft of stream 1 or stream 2 is bounded above by d_{max}, i.e.

$$\left|d_i^k\right| \leq d_{max}, \quad \text{with} \quad d_{max} = \frac{d}{\cos\phi} = \frac{d}{\sin\frac{\theta}{2}}. \quad (3)$$

At any given time, its position (x_i^k, y_i^k) is then a function of its initial position (x_{i0}, y_{i0}), which is the same for all the aircraft in a given flow, its speed v, its lateral deviation d_i^k and the time t_i^k between the current instant and the instant when it entered the conflict area and did its avoidance maneuver.

"Open-loop" Modeling of the Encounter Behavior

In this section, we present an analytical method to determine the probability of conflict between aircraft as a function of the flows characteristics only, i.e. the crossing angle and the inter-arrival time probability density function (PDF) of each flow, without considering the conflict avoidance algorithm presented in the preceding section. This approach is then similar to previous works such as [7, 8, 9, 10, 11], even if it is a simplified approach. We call it an "open-loop" approach since no controller influence is taken into account to determine the probability of conflict. On the contrary, the "closed-loop" approach consider the avoidance algorithm in the feedback loop to determine this probability: this is what happens in the real life or in simulations. The interest of this section is to compare both approaches (as illustrated by Figures 1 and 2).

Probability of Conflict

We consider an aircraft AC_1^1 entering the conflict management area at time t_0. We want to determine the probability that AC_1^1 has no conflict with any aircraft as a function of the geometry of the encounter (i.e. the crossing angle) and the characteristics of the flows (i.e. the aircraft speed v and the probability density function of the inter-arrival time between aircraft $f_{\Delta T_i}(\Delta t_i)$). Let $P_{NC}(AC_1^1)$ be this probability of no conflict (or probability of absence of conflict). We only detail the case of AC_1^1 entering the conflict management area $\mathscr{C}$, but a similar argument would apply to AC_2^1 entering $\mathscr{C}$ and would lead to $P_{NC}(AC_2^1)$.

Since the aircraft AC_1^1 just entered $\mathscr{C}$, its position is (x_{10}, y_{10}). Many aircraft from flow 2 (and flow 1) have already entered the conflict area, and some of them have already left it. Indeed, there is no chance that AC_1^1 be in a conflict with an aircraft from its own flow. Therefore, the probability density function $f_{\Delta T_i}(\Delta t_i)$ is such that Δt_i has a minimum value Δt_i^{min}, with $\Delta t_i^{min} \geq \frac{d}{v}$. Since no avoidance maneuver is allowed, $P_{NC}(AC_1^1)$ is then the probability that there is no aircraft from flow 2 in the segment S_2^0. From now on, we use the notation (AC_2^k i.c. AC_1^1) for "AC_2^k is in conflict with AC_1^1" and (AC_2^k n.i.c. AC_1^1) for "AC_2^k is not in conflict with AC_1^1". If AC_2^1 n.i.c. AC_1^1, there is no chance that AC_2^k i.c. AC_1^1, $k \geq 2$. Only AC_2^1 needs to be taken into account to

determine $P_{NC}(AC_1^1)$. Determining $P_{NC}(AC_1^1)$ is then equivalent to determining $P(AC_2^1 \text{ n.i.c. } AC_1^1)$, or in another term

$$\begin{aligned} P_{NC}(AC_1^1) &= P(AC_2^1 \text{ n.i.c. } AC_1^1) \\ &= P(AC_2^1 \notin S_2^0). \end{aligned}$$

The "age" t_2^1 of the aircraft AC_2^1 is the time elapsed between its entry in the conflict management area and t_0. Regarding AC_2^1, the probability density function of its age t_2^1, $f_{T_2^1}(t_2^1)$, is given by the following expression (see [22] for details):

$$f_{T_2^1}(t_2^1) = \begin{cases} \lambda_2^m & \text{when} \quad 0 \leq t_2^1 \leq \Delta t_2^{min} \\ \lambda_2^m(1-F_{\Delta T_2}) & \text{when} \quad \Delta t_2^{min} \leq t_2^1, \end{cases} \tag{4}$$

where $\frac{1}{\lambda_2^m}$ is the mean of $f_{\Delta T_2}(\Delta t_2)$ and $F_{\Delta T_2}$ is the distribution function of the inter-arrival time of flow 2 associated to $f_{\Delta T_2}$.

Using the conditions on the absence of conflict (1)–(2), the probability $P(AC_2^1 \notin S_2^0)$ can be written

$$\begin{aligned} &P(AC_2^1 \notin S_2^0) \\ &= 1 - P(-x_{10}\tan\phi + y_{10} - \frac{d}{\cos\phi} \leq -x_2^1\tan\phi + y_2^1 \\ &\qquad \leq -x_{10}\tan\phi + y_{10}). \end{aligned} \tag{5}$$

The position of the aircraft AC_2^1, (x_2^1, y_2^1), is a function of the encounter configuration and its age:

$$x_2^1 = x_{20} + v\cos\theta t_2^1 \tag{6}$$

$$y_2^1 = y_{20} - v\sin\theta t_2^1. \tag{7}$$

Replacing (6)–(7) into (5), we obtain

$$P(AC_2^1 \text{ n.i.c. } AC_1^1) = 1 - P(L_n \leq -t_2^1 \leq L_z), \tag{8}$$

where

$$L_n = \frac{(x_{20}-x_{10})\tan\phi + y_{10} - y_{20} - d_{max}}{v(\cos\theta\tan\phi + \sin\theta)}$$

$$L_z = \frac{(x_{20}-x_{10})\tan\phi + y_{10} - y_{20}}{v(\cos\theta\tan\phi + \sin\theta)}.$$

A simple geometrical analysis leads to

$$(x_{20}-x_{10})\tan\phi + y_{10} - y_{20} = 0.$$

Equation (17) can then be written as

$$P(AC_2^1 \text{ n.i.c. } AC_1^1) = 1 - P(L_n \leq -t_2^1 \leq 0), \tag{9}$$

where

$$L_n = \frac{-d_{max}}{v(\cos\theta\tan\phi + \sin\theta)}.$$

Considering the random variable M with its associated PDF $f_M(m)$ and two scalars a, b, we recall the PDF of the new variable $N = aM + b$ (see [22]):

$$f_N(n) = \frac{1}{|a|} f_M(\frac{m-b}{a}). \tag{10}$$

Using (10) and (4), we can determine the probability density function of "$-t_2^1$", $f_{-T_2^1}(-t_2^1)$. The probability $P(AC_2^1 \text{ n.i.c. } AC_1^1)$ can then be determined using

$$P(AC_2^1 \text{ n.i.c. } AC_1^1) = \int_{L_n}^{L_p} f_{-T_2^1}(-t_2^1)d(-t_2^1).$$

Knowing $P_{NC}(AC_1^1)$ (or $P_{NC}(AC_2^1)$) and the flows characteristics, it is easy to compute the probability of conflict for the considered intersection I within a time frame T, $P_C^T(I)$.

Comparison With Simulations

We compare the probability of no conflict $P_{NC}(AC_1^1)$ and $P_{NC}(AC_2^1)$ determined by the preceding analysis ("open-loop" approach) with the probabilities of conflict given by the simulation results considering the automated conflict resolution presented in the modeling section ("closed-loop" approach). The PDF of the inter-arrival time is modeled as an exponential distribution with a minimal value, which is a quite realistic model (see for instance [23, 24]):

$$f_{\Delta T_i}(\Delta t_i) = \begin{cases} \lambda_i^m e^{-\lambda_i^m(\Delta t_i - \Delta t_i^{min})} & \text{when } \Delta t_i \geq \Delta t_i^{min} \\ 0 & \text{when } 0 \leq \Delta t_i < \Delta t_i^{min}, \end{cases} \tag{11}$$

i=1,2. For clarity, we deal in this results analysis with inter-arrival distance Δd_i instead of inter-arrival time Δt_i, i.e. we consider $\Delta d_1^{min} = v\Delta t_i^{min}$ and $d_i^m = \frac{v}{\lambda_i^m}$. We run the simulations with the following encounter and flows characteristics:

- $\theta = 90°$
- $\mathscr{C} \equiv \text{circle}(\text{O}, 100\text{NM})$
- 500 aircraft in each flow
- $v = 450\text{kt}$
- $\Delta d_1^{min} = \Delta d_2^{min} = 5\text{NM}$
- $\text{range}(d_1^m) = \text{range}(d_2^m) = [0.5, 49.5]\text{NM}$.

We plot the probabilities of no conflict $P_{NC}(AC_1^1)$ and $P_{NC}(AC_2^1)$ from the preceding analysis and from simulations on Figures 4 and 5: these probabilities are functions of the mean inter-arrival distance between aircraft from the same flow d_i^m. Considering realistic values of d_i^m ($d_i^m \geq 35$NM), we see that both methods give very similar results: this statement justifies the usual "open-loop approach" developed in this section, which does not take into account the influence of the conflict avoidance algorithm. It also validates other works that follow that the same kind of "open-loop" method, such as [8, 9, 10, 11, 7]. Complexity maps can then be rapidly generated for the considered encounter configuration and flow characteristics : these complexity maps give the probability of non conflict (or conflict) at the intersection point. The same approach can easily deal with multiple flows intersections, even in three dimensions, leading to complexity maps of realistic airspaces (see [7] for instance). With this approach, we can also see immediately the consequences of the chosen configuration (routes and flow rates) on the probability of conflict, considered as a measure of the airspace complexity. Moreover, human factors can be taken into account quite easily with this approach. Indeed, an important limitation when considering human air traffic controllers is the number of conflicts that can be solved per unit of time: time is needed to see that there is a conflict, to choose the right maneuver, to contact the aircraft involved in the conflict, to give them the maneuver order and to be sure that it is well understood and followed. The probability of conflict at the intersection I per T minutes $P_C^T(I)$ is expressed easily as a function of the encounter characteristics. For instance, Figures 4 and 5 directly show how increasing the flow rate increases the probability of conflict. If necessary, the air traffic manager can modify the flow rates or the crossing angle to decrease the controller workload.

Nevertheless, the preceding "open-loop" approach suffers from some limitations. First we can notice a difference between the analytical and the simulations results at high flow rates: the probability of conflict determined by both methods are quite different (see Figures 4 and 5 when the mean inter-arrival distances d_1^m and d_2^m are small). Moreover, the "open-loop" approach does not take into account how the conflict resolution area may affect the area surrounding the considered intersection. Indeed, aircraft make a lateral deviation

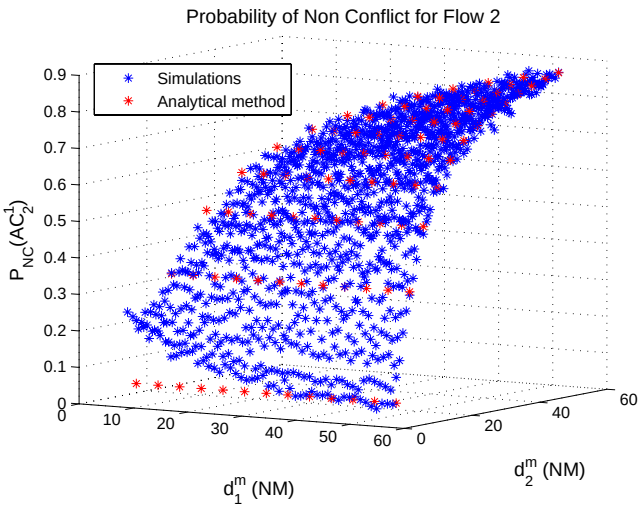

Figure 4: Probability of Absence of Conflict for Flow 2

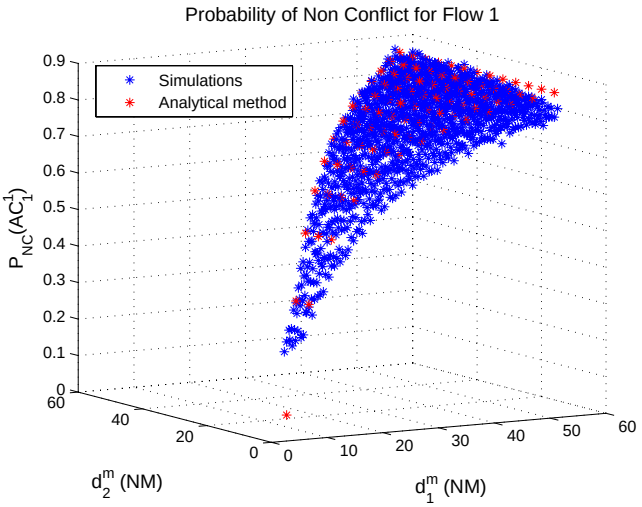

Figure 5: Probability of Absence of Conflict for Flow 1

when a conflict occurs, thereby spreading the initial flow until aircraft resume their initial trajectory. The spread of the aircraft flow may create others conflicts with adjacent flows that do not exist if we only consider the initial track. To illustrate this point, we plot the Cumulative Distribution Function (CDF) of the lateral deviation for each flow as a function of the inter-arrival distance (see Figures 6 and 7). From these plots, we recover the maximum lateral deviation $d_{max} = \dfrac{d}{\cos\phi} = 7$NM. Even considering the "best scenario" ($\theta = 90°$), the lateral deviation is important and needs to be taken into account in the encounter modeling. We also recover the probability of absence of conflict (see Figures 4 and 5) that corresponds to the vertical lines (i.e. a 0NM lateral

deviation since there is no conflict). A dissymmetry can also be noticed between the positive and negative lateral deviation. In other terms, the aircraft tend to move to the other flow to prevent a conflict.

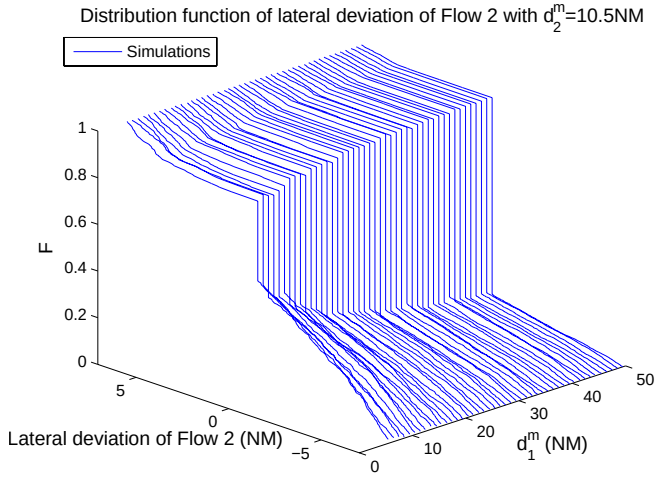

Figure 6: CDF of the Lateral Deviation of Flow 2

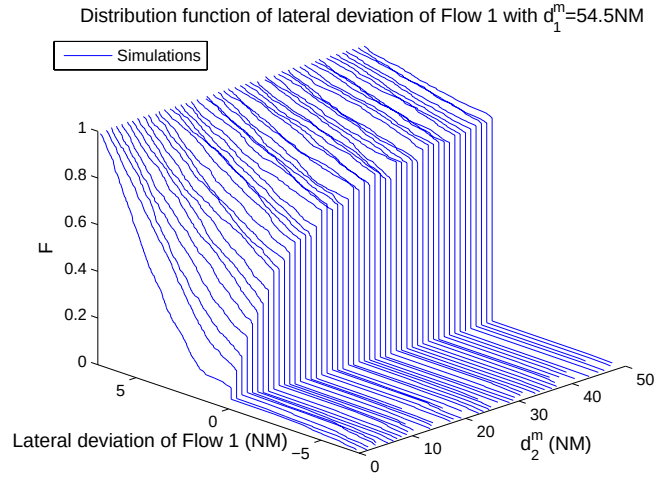

Figure 7: CDF of the Lateral Deviation of Flow 1

"Closed-loop" Modeling of the Encounter Behavior

In this section, we present an analytical method to model the "closed-loop" behavior of the encounter, taking into account the automated conflict resolution, and then bypassing the previous limitations of the "open-loop" approach. The model determines the probability of conflict and gives a good idea of the spatial distribution of the aircraft as a function of the encounter configuration and flows characteristics.

Probability of conflict

As in the "open-loop" section, we consider the aircraft AC_1^1 entering the conflict management area at time t_0. We use the same notations. Due to the conflict avoidance algorithm (the offset method), AC_1^1 is subject to a lateral deviation d_1^1 ($d_1^1 = 0$ if there is no conflict). Only a few aircraft need to be taken into account to determine $P_{NC}(AC_1^1)$. Indeed, there is no chance that AC_1^1 be in a conflict with an aircraft from its own flow and with an aircraft from flow 2 as soon as it reached the straight line D^d defined in Fig. 3. From Fig. 3, we find that the maximum number of aircraft N_2 (only from flow 2) that AC_1^1 may be in conflict with is

$$N_2 = \frac{d}{v\Delta t_2^{min} \sin\phi}.$$

Let N_2^{max} be the number of aircraft that have entered the conflict area at the considered time t_0. The "age" t_2^k of the aircraft AC_2^k, $k = 1,\ldots,N_2^{max}$, is the time elapsed between its entry in the conflict area (and then its conflict avoidance maneuver) and t_0. The probability density function of the age of AC_2^1, $f_{T_2^1}(t_2^1)$, is given by (4). Considering two independent random variables M,N with their associated PDF $f_M(m), f_N(n)$, we recall the PDF of the new variable $Z = M+N$:

$$f_Z(z) = f_M * f_N(z) = \int_{-\infty}^{\infty} f_M(y) f_N(z-y) dz. \qquad (12)$$

Considering now the aircraft AC_2^k, the probability density function of its age t_2^k, $f_{T_2^k}(t_2^k)$, can then be determined by the convolution between $f_{T_2^{k-1}}$ and $f_{\Delta T_2}$, for $k \geq 2$ (applying Equation (12), since the inter-arrival time between any two aircraft are independent variables). In other terms, we have

$$f_{T_2^k} = f_{T_2^{k-1}} * f_{\Delta T_2}. \qquad (13)$$

The probability of conflict we want to determine, $P_{NC}(AC_1^1)$, can be expressed as follows:

$$\begin{aligned} P_{NC}(AC_1^1) &= P(\forall k, AC_2^k \text{ n.i.c. } AC_1^1) \\ &\simeq \prod_{k=1}^{N_2} P(AC_2^k \text{ n.i.c. } AC_1^1). \end{aligned}$$

The last equation assumes the independence of the considered probabilities. This assumption seems reasonable

from a physical viewpoint, since there is no possible conflict between aircraft within the same flow and independence of inter-arrival time. So we have

$$P_{NC}(AC_1^1) = \prod_{k=1}^{N_2} \big(1 - P(AC_2^k \text{ i.c. } AC_1^1)\big). \quad (14)$$

The N_2 aircraft from flow 2, AC_2^k, $k = 1, \ldots, N_2$, that need to be taken into account to determine $P_{NC}(AC_1^1)$ have already performed a lateral deviation d_2^k. So the position of the aircraft AC_2^k at time t_0 is

$$x_2^k = x_{20} + v\cos\theta t_2^k + d_2^k \sin\theta \quad (15)$$

$$y_2^k = y_{20} - v\sin\theta t_2^k - d_2^k \cos\theta. \quad (16)$$

Replacing (15)–(16) into (5), we obtain

$$P(AC_2^k \text{ i.c. } AC_1^1) = P(L_n \le s_2 d_2^k - t_2^k \le L_p), \quad (17)$$

where

$$s_2 = \frac{-\sin\theta\tan\phi - \cos\theta}{v(\cos\theta\tan\phi + \sin\theta)}$$

$$L_n = \frac{-d_{max}}{v(\cos\theta\tan\phi + \sin\theta)}$$

$$L_p = \frac{d_{max}}{v(\cos\theta\tan\phi + \sin\theta)}.$$

The probability density function of the age of the aircraft, $f_{T_2^k}(t_2^k)$, is known. The probability density function of the lateral deviation $f_{D_2^k}(d_2^k)$ is modeled as illustrated by Figure 8: $f_{D_2^k}(d_2^k)$ is a function of two parameters α_2 ($\equiv$ probability of non conflict) and β_2 (balance between the positive and negative lateral deviation). According to the associated distribution function depicted in Figures 6 and 7, this model seems adequate. Indeed, the PDF obtained by computing the derivative of the CDF from simulations can be quite well approximated by the proposed model. In particulary, the dissymmetry between the positive and negative lateral deviation that appears in Figures 6 and 7 (i.e. each flow tends to move towards the other flow to avoid a conflict, especially at high flow rates difference) would be taken into account using this model.

Introducing the new variable $z_2^k = s_2 d_2^k - t_2^k$ and applying Equation (12), its PDF writes then

$$f_{Z_2^k} = f_{s_2 D_2^k} * f_{-T_2^k}, \quad (18)$$

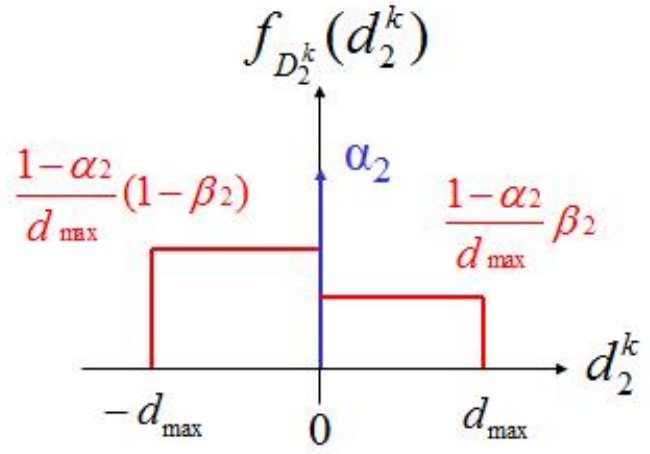

Figure 8: Model of the Lateral Deviation PDF of Flow 2

where $f_{s_2 D_2^k}(s_2 d_2^k)$ and $f_{-T_2^k}(-t_2^k)$ can be determined using (10) and assuming that the lateral deviation and the age of the aircraft are independent variables. According to (14), the probability of absence of conflict $P(AC_2^k \text{ i.c. } AC_1^1)$ is then written

$$P(AC_2^k \text{ i.c. } AC_1^1) = \int_{L_n}^{L_p} f_{Z_2^k}(z_2^k) d(z_2^k). \quad (19)$$

In order to compute α_2 and β_2, we decompose the PDF of the lateral deviation $f_{D_2^k}(d_2^k)$ into 3 sub-PDFs defined by

$$\begin{aligned} f_{D_{2p}^k}(d_2^k) &= \begin{cases} 1 & \text{when} \quad 0 < d_2^k \le d_{max} \\ 0 & \text{otherwise} \end{cases} \\ f_{D_{2\delta}^k}(d_2^k) &= \delta(d_2^k) \\ f_{D_{2n}^k}(d_2^k) &= \begin{cases} 1 & \text{when} \quad -d_{max} \le d_2^k < 0 \\ 0 & \text{otherwise.} \end{cases} \end{aligned} \quad (20)$$

We then define 3 corresponding PDF $f_{Z_{2\gamma}^k}(z_2^k)$, $\gamma = \{n, \delta, p\}$, where $z_2^k = s_2 d_2^k - t_2^k$. According to the model depicted on Figure 8, Equation (19) can be rewritten

$$\begin{aligned} P(AC_2^k \text{ i.c. } AC_1^1) = &\frac{(1-\alpha_2)(1-\beta_2)}{d_{max}} \int_{L_n}^{L_p} f_{Z_{2n}^k}(z_2^k) d(z_2^k) \\ &+ \alpha_2 \int_{L_n}^{L_p} f_{Z_{2\delta}^k}(z_2^k) d(z_2^k) \\ &+ \frac{(1-\alpha_2)\beta_2}{d_{max}} \int_{L_n}^{L_p} f_{Z_{2p}^k}(z_2^k) d(z_2^k). \end{aligned} \quad (21)$$

Since the probability of non conflict for $P_{NC}(AC_1^1)$ is in fact equal to α_1, we have the equation

$$\alpha_1 = \prod_{k=1}^{N_2} \big(1 - P(AC_2^k \text{ i.c. } AC_1^1)\big), \tag{22}$$

where $P(AC_2^k \text{ i.c. } AC_1^1)$ is a function of α_2, β_2 (see (21)).

Similarly, we find from Fig. 8

$$(1-\alpha_1)(1-\beta_1) = 1 - \prod_{k=1}^{N_2} \big(1 - P(AC_2^k \in \mathscr{A}_2^{up})\big), \tag{23}$$

where $P(AC_2^k \in \mathscr{A}_2^{up})$ is the probability that the aircraft AC_2^k belongs to the area $\mathscr{A}_2^{up}$ shown in Figure 3. This probability can be written

$$P(AC_2^k \in \mathscr{A}_2^{up}) = \frac{(1-\alpha_2)(1-\beta_2)}{d_{max}} \int_0^{L_p} f_{Z_{2n}^k}(z_2^k) d(z_2^k). \tag{24}$$

The equations (22) and (23), with the considered probabilities defined by (21) and (24), give a system of two equations as a function of the 4 parameters α_i, β_i, $i = 1,2$.

Following the same approach and considering the dual case, i.e. AC_2^1 entering the conflict area, we obtain the following equations:

$$\alpha_2 = \prod_{k=1}^{N_1} \big(1 - P(AC_1^k \text{ i.c. } AC_2^1)\big) \tag{25}$$

with

$$\begin{aligned} P(AC_1^k \text{ i.c. } AC_2^1) = & \frac{(1-\alpha_1)(1-\beta_1)}{d_{max}} \int_{L_n}^{L_p} f_{Z_{1n}^k}(z_1^k) d(z_1^k) \\ & + \alpha_1 \int_{L_n}^{L_p} f_{Z_{1\delta}^k}(z_1^k) d(z_1^k) \\ & + \frac{(1-\alpha_1)\beta_1}{d_{max}} \int_{L_n}^{L_p} f_{Z_{1p}^k}(z_1^k) d(z_1^k), \end{aligned} \tag{26}$$

and

$$(1-\alpha_2)\beta_2 = 1 - \prod_{k=1}^{N_1} \big(1 - P(AC_1^k \in \mathscr{A}_1^{up})\big) \tag{27}$$

with

$$P(AC_1^k \in \mathscr{A}_1^{up}) = \frac{(1-\alpha_1)\beta_1}{d_{max}} \int_0^{L_p} f_{Z_{1n}^k}(z_1^k) d(z_1^k). \tag{28}$$

Comparison With Simulations

The preceding equations yield a system of four equations as a function of the 4 parameters $\alpha_i, \beta_i, i = 1,2$ we want to determine. This system can be solved in real time using commonly available numerical solvers. We use the *fsolve* function of Matlab with the default optimization parameters. In order to compare our analytical results with simulations results, we use the same simulation setup as in the "open-loop" section.

We plot the probabilities as a function of the mean inter-arrival distance between aircraft from the same flow d_i^m. In Figures 9 and 10, we see that the plots from the simulations and the analytical method are very similar for realistic flow rates characteristics ($d_i^m \geq 35$NM). Even if there is still a difference at high flow rates, the plots tend to match better than in the "open-loop" section, as illustrated in Fig. 11.

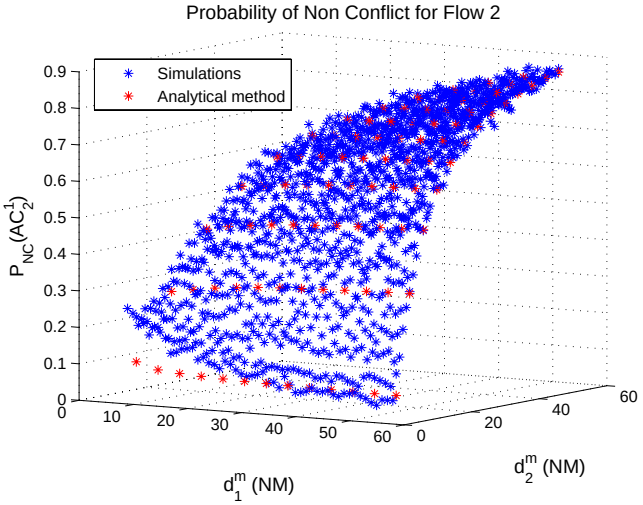

Figure 9: Probability of Absence of Conflict for Flow 2

We plot the distribution function of the lateral deviation for each flow as a function of the inter-arrival distance on Figures 12 and 13. The graphs from the analytical method and the simulations are very similar. Especially, we recover the dissymmetry between the positive and negative lateral deviation, and the shape of how the flows spread around their initial tracks: this is the main advantage in comparison to the "open-loop" approach.

Conclusion and Future Works

In this paper, we have presented a new methodology to rapidly generate probability density functions of

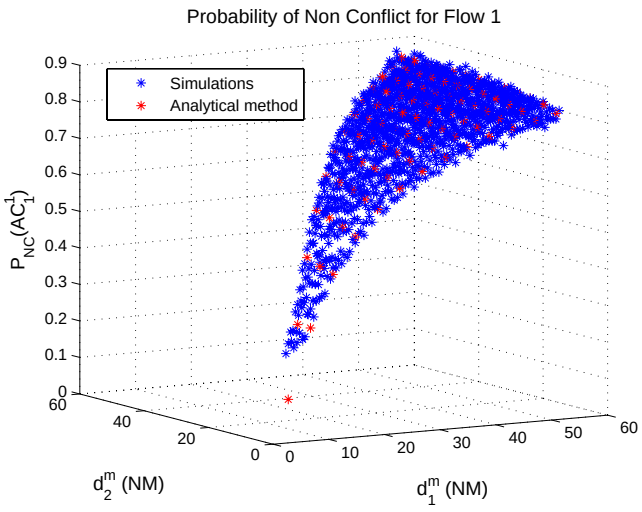

Figure 10: Probability of Absence of Conflict for Flow 1

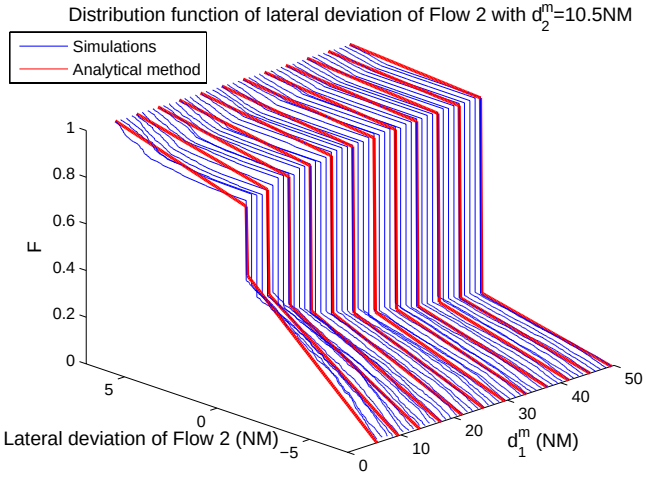

Figure 12: CDF of the Lateral Deviation of Flow 2

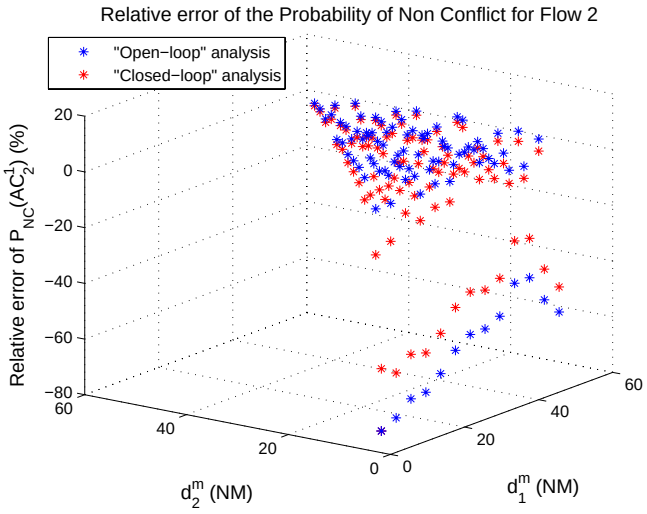

Figure 11: Relative Error of the Probability of No Conflict for Flow 2

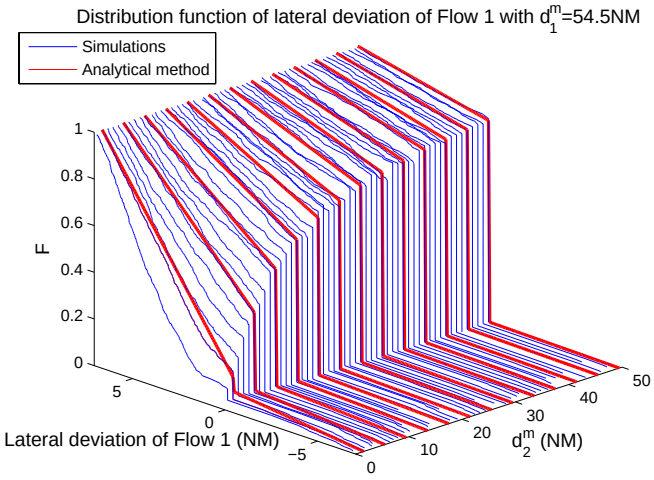

Figure 13: CDF of the Lateral Deviation of Flow 1

aircraft position under "closed-loop" control policies at a pair-wise intersection level, as functions of the encounter and flow rates characteristics. This method can lead to determine complexity maps built from the probability of conflict between aircraft, as well as the flow spread due to avoidance maneuvers. Through simulations, we also highlighted how our "closed-loop" model bypasses the limitations of the usual "open-loop" approach that considers only on the structure of the conflict.

Considering the influence of the conflict avoidance algorithm to estimate the probability of conflict and then to compute complexity maps is really important at the sector level. Indeed, deconflicting a pair-wise intersection may affect the surrounding area and then create new conflicts that must be taken into account. To illustrate this point, we consider the Cleveland sector as shown in Figures 14 and 15 and we draw at each intersection the circles with centers the crossing points and with radius d_{max} (the real aircraft spatial distribution at the intersection level should be one rectangle for each flow, but we draw circles for clarity). We see that several circles overlap, even if the crossing points of the corresponding intersections are far. These overlapping areas mean that an avoidance maneuver at one intersection may cause a secondary conflict with an aircraft involved in the other intersection.

We currently work on extending the approach proposed in this paper to the sector level. The first step will be to give a similar complexity map at the intersection

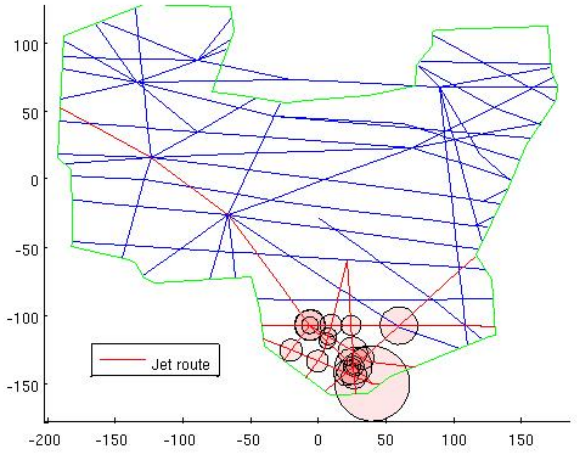

Figure 14: Cleveland Center

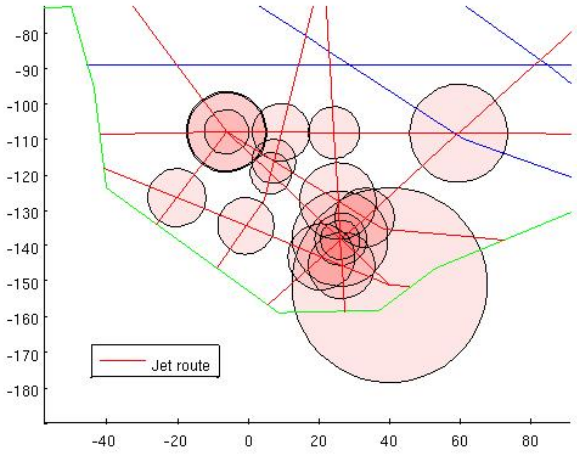

Figure 15: Zoom-in on the Considered Sector

level considering N flows, as it may appear in a real routes configuration. Then we will need to compute the probability of presence of two aircraft from two different intersections in the overlapping areas (shown in Fig. 15). It will be interesting and useful to follow the same methodology considering another conflict resolution method (heading or/and speed change), and to compare the generated complexity maps for a given traffic configuration.

References

[1] Joint Planning and Development Office. Next generation air transportation system integrated work plan: A functional outline. Technical report, Joint Planning and Development Office, Washington, DC, September 2008.

[2] I.V. Laudeman, S.G. Shelden, R. Branstrom, and C.L. Brasil. Dynamic density: An air traffic management metric. *Ames Research Center-112226*, 1998.

[3] B. Sridhar, K.S. Sheth, and S. Grabbe. Airspace complexity and its application in air traffic management. In *2 nd USA/Europe Air Traffic Management R&D Seminar*, 1998.

[4] D. Delahaye, S. Puechmorel, J. Hansman, and J. Histon. Air traffic complexity based on non linear dynamical systems. In *USA-Europe ATM R&D Seminar*, 2003.

[5] D. Delahaye, S. Puechmorel, J. Hansman, and J. Histon. Air traffic complexity map based on non linear dynamical systems. *Air Traffic Control Quarterly*, 12(4):367–390, 2004.

[6] A. Yousefi and G.L. Donohue. Temporal and Spatial Distribution of Airspace Complexity for Air Traffic Controller Workload-Based Sectorization. In *AIAA Guidance, Navigation, and Control Conf., San Francisco, CA*, pages 6455–6468, 2004.

[7] M. Prandini, V. Putta, and J. Hu. A probabilistic measure of air traffic complexity in three-dimensional airspace. *Int. J. Adapt. Control Signal Process*, 1:1–25, 2009.

[8] R.A. Paielli and H. Erzberger. Conflict probability estimation for free flight. *Journal of Guidance, Control, and Dynamics*, 20(3):588–596, 1997.

[9] R. Irvine. A simplified approach to conflict probability estimation. In *Proc. of the 20th Digital Avionics Systems Conference*, volume 2, pages 7F5/1–7F5/12, 2001.

[10] R. Irvine. A geometrical approach to conflict probability estimation. *Air Traffic Control Quarterly*, 10(2):85–113, 2002.

[11] H.A.P. Blom, G.J. Bakker, M.H.C. Everdij, and M.N.J. Van der Park. Collision risk modeling of air traffic. In *Proceedings of European Control Conference*, 2003.

[12] H.A.P. Blom and G.J. Bakker. Conflict probability and incrossing probability in air traffic management. In *Proc. of the 41st IEEE Conference on Decision and Control*, volume 3, pages 2421–2426, 2002.

[13] Z.-H. Mao and E. Feron. Stability and performance of intersecting aircraft flows under sequential conflict resolution. In *Proc. 2001 American Control Conference*, 2001.

[14] K. Treleaven and Z.-H. Mao. Conflict Resolution and Traffic Complexity of Multiple Intersecting Flows of Aircraft. *IEEE Transactions on Intelligent Transportation systems*, 9(4):633–643, 2008.

[15] M. Gariel and E. Feron. Graceful Degradation of Air Traffic Operations: Airspace Sensitivity to Degraded Surveillance Systems. *Proceedings of the IEEE*, 96(12):2028–2039, 2008.

[16] L. Pallottino, E. Feron, and A. Bicchi. Conflict resolution problems for air traffic management systems solved with mixed integer programming. *IEEE Transactions on Intelligent Transportation Systems*, 3, 2002.

[17] A. Vela, S. Solak, W. Singhose, and J.-P. Clarke. A mixed integer program for flight-level assignment and speed control for conflict resolution. In *Proc. of the 2009 Conference on Decision and Control*, 2009.

[18] A. Vela, E. Salaün, S. Solak, E. Feron, W. Singhose, and J.-P. Clarke. A two-stage stochastic optimization model for air traffic conflict resolution under wind uncertainty. In *Proc. of the 28th Digital Avionics Systems Conference*, 2009.

[19] K. Lee, E. Feron, and A. Pritchett. Air traffic complexity: An input-output approach. In *American Control Conference, 2007*, pages 474–479, 2007.

[20] K. Lee, E. Feron, and A. Pritchett. Describing Airspace Complexity: Airspace Response to Disturbances. *Journal of Guidance, Control, and Dynamics*, 32(1), 2009.

[21] Z.-H. Mao, E. Feron, and K. Bilimoria. Stability and performance of intersecting aircraft flows under decentralized conflict avoidance rules. *IEEE Transactions on Intelligent Transportation Systems*, 2(2):101–109, 2001.

[22] S.M. Ross. *Stochastic processes*. Wiley series in probability and mathematical statistics, second edition, 1996.

[23] D. Moreau and S. Roy. A stochastic characterization of en route traffic flow management strategies. In *Proc. of the AIAA Guidance, Navigation, and Control Conference*, pages 6274–6285, 2005.

[24] J-P.B. Clarke, S. Solak, Y.-H. Chang, L. Ren, and A.E. Vela. Air trafic Flow Management in the Presence of Uncertainty. In *USA-Europe ATM R&D Seminar*, 2009.

Acknowledgments

This work is funded by NASA under Grant NNX08AY52A and the FAA under Award No. 07-C-NE-GIT, Amendment Nos. 005, 010, and 020.

Email Addresses

Erwan Salaün: erwan.salaun@gatech.edu,
Adan Vela: aevela@gatech.edu,
Eric Feron: feron@gatech.edu,
John-Paul Clarke: johnpaul@gatech.edu,
Senay Solak: solak@som.umass.edu.

28th Digital Avionics Systems Conference
October 25-29, 2009